

Autocrine Platelet-derived Growth Factor-Vascular Endothelial Growth Factor Receptor-related (Pvr) Pathway Activity Controls Intestinal Stem Cell Proliferation in the Adult *Drosophila* Midgut^{*[5]}

Received for publication, May 3, 2012, and in revised form, June 20, 2012. Published, JBC Papers in Press, June 21, 2012, DOI 10.1074/jbc.M112.378018

David Bond and Edan Foley¹

From the Department of Medical Microbiology and Immunology, University of Alberta, Edmonton, Alberta T6G 2S2, Canada

Background: *Drosophila* midgut intestinal stem cells (ISCs) proliferate and differentiate to replace mature cell types and maintain tissue integrity.

Results: The Pvr signal transduction pathway provides an autocrine control of the differentiation of ISCs into mature cells.

Conclusion: The Pvr pathway is an intrinsic regulator of ISC differentiation.

Significance: Pvr is the first strictly intrinsic regulator of ISC differentiation characterized.

A dynamic pool of undifferentiated somatic stem cells proliferate and differentiate to replace dead or dying mature cell types and maintain the integrity and function of adult tissues. Intestinal stem cells (ISCs) in the *Drosophila* posterior midgut are a well established model to study the complex genetic circuitry that governs stem cell homeostasis. Exposure of the intestinal epithelium to environmental toxins results in the expression of cytokines and growth factors that drive the rapid proliferation and differentiation of ISCs. In the absence of stress signals, ISC homeostasis is maintained through intrinsic pathways. In this study, we uncovered the PDGF- and VEGF-receptor related (Pvr) pathway as an essential regulator of ISC homeostasis under unstressed conditions in the posterior midgut. We found that Pvr is coexpressed with its ligand Pvf2 in ISCs and that hyperactivation of the Pvr pathway distorts the ISC developmental program and drives intestinal dysplasia. In contrast, we show that mutant ISCs in the Pvf/Pvr pathway are defective in homeostatic proliferation and differentiation, resulting in a failure to generate mature cell types. Additionally, we determined that extrinsic stress signals generated by enteropathogenic infection are epistatic to the hypoplasia generated in Pvf/Pvr mutants, making the Pvr pathway unique among all previously studied intrinsic pathways. Our findings illuminate an evolutionarily conserved signal transduction pathway with essential roles in metazoan embryonic development and direct involvement in numerous disease states.

Stem cells are undifferentiated, proliferatively competent cells that provide a constant source of mature cell types essential for normal tissue growth and maintenance (1). In adult tissues, somatic stem cells replace a multitude of terminally differentiated cells and expand in response to extrinsic cues to

confer plasticity on organ size and cell numbers (1). Stem cell homeostasis is maintained through a delicate balance of stem cell intrinsic and extrinsic signals that orchestrate proliferation and/or differentiation in response to tissue requirements (2). When regulatory systems that control stem cell homeostasis fail, impaired tissue function and organ failure result. In the extreme, breakdown of stem cell proliferative controls can lead to aberrant mitosis and the development of cancers (3). Stem cells and cancers share striking similarities in that both are pluripotent and have exceptional proliferative potential (1). Therefore, unraveling the complex signaling networks that control stem cell homeostasis not only aids our comprehension of normal tissue growth and repair but can also profoundly impact our understanding of cancer development and progression.

The recent discovery of stem cells in the posterior midgut of adult *Drosophila melanogaster* presents a remarkable system to explore factors that regulate stem cell homeostasis (4, 5). This is due to the unequaled genetic tractability of the *Drosophila* model and the overarching similarities between *Drosophila* and mammalian intestinal cell types, morphology, developmental patterning, and signaling interactions (2, 6, 7). In the *Drosophila* posterior midgut (functional equivalent of the human small intestine) (2, 5, 8), intestinal stem cells (ISCs)² self-renew by mitosis and differentiate into nonproliferative, undifferentiated enteroblasts (EBs). In turn, EBs differentiate into mature epithelial enterocytes (ECs) or secretory enteroendocrine cells (EEs) (7). Posterior midgut ISCs lie in close contact with the underlying basal lamina established by a meshwork of visceral muscle cells (5, 9). Upon ISC division, asymmetric Delta (DI) expression directs differential Notch (N) signals between the newly formed ISC/EB equivalence group to establish developmental fate through lateral inhibition (10). The basally located DI positive daughter cell within the niche retains stem cell iden-

* This work was supported by Canadian Institute for Health Research Grant MOP 77746 and a Alberta Innovates Health Solutions grant.

[5] This article contains supplemental Fig. S1.

¹ To whom correspondence should be addressed: Dept. of Medical Microbiology and Immunology, University of Alberta, Edmonton, AB T6G 2S2, Canada. Tel.: 780-492-0935; Fax: 780-492-7521; E-mail: efoley@ualberta.ca.

² The abbreviations used are: ISC, intestinal stem cell; EB, enteroblast; EC, enterocyte; EE, enteroendocrine cell; DI, Delta; N, Notch; dJNK, *Drosophila* JNK; EGFR, EGF receptor; MARCM, mosaic analysis with a repressible cell marker; NRE, Notch reporter element; pH3, phospho-H3; PDGFR, PDGF receptor.

Pvr Regulates *Drosophila* Midgut Homeostasis

tity, whereas the opposing N positive daughter cell differentiates into an EB (5, 10). The intensity of N signals continues to control EB fate decisions, because high N signals in EBs drive differentiation into mature ECs, whereas low N signals promote the EE cell fate (11, 12). Large, polyploid ECs are the predominant terminally differentiated cell type in the gut and overlie the ISC/EBs to form a continuous intestinal epithelial monolayer through which nutrients are absorbed. Secretory EEs are found interspersed throughout the intestinal epithelium and are primarily concerned with secretion of regulatory peptides.

The developmental architecture discussed above adequately describes the controls that ensure orderly replenishment of dead epithelial cells under steady state conditions. However, a true genetic evaluation of intestinal integrity must appreciate the intestines as a major interface between an animal and its environment, with intestines continuously exposed to a revolving and unpredictable carousel of pathogenic microbes and toxic molecules. Therefore, modifiable proliferative mechanisms are crucial to ensure epithelial integrity after the ingestion of cytotoxic agents or enteric pathogens. Not surprisingly, *Drosophila* ISCs use intricate and partially overlapping cell signaling networks that integrate cell intrinsic and extrinsic cues to coordinate tissue homeostasis and maintain midgut epithelial integrity (13). Exposure to cytotoxic or infectious agents, such as the pathogenic bacterium *Pseudomonas entomophila*, rapidly increases ISC mitoses by 10–100-fold to replace dead and dying epithelial cells (14, 15). These proliferative responses are largely initiated by activation of ISC extrinsic pathways, such as Jak/Stat, *Drosophila* JNK (dJNK), and Yorkie/Warts (13, 14, 16–20). For example, cytotoxic and infectious agents that stress or damage ECs induce the expression of numerous cytokines and growth factors such as Upd (unpaired) cytokines from ECs, and EGF-like ligands from visceral muscle (14, 17, 21, 22). Combined, these factors engage their cognate receptor on ISCs to promote JAK/STAT and EGF receptor (EGFR) pathways, respectively. These extrinsic signals are then integrated in the ISCs to orchestrate appropriate proliferative and differentiation mechanisms (13, 18).

In the absence of extrinsic challenges, ISCs turnover proceeds slowly. The rate of ISC turnover in females is twice that of males, completely regenerating the midgut epithelium in approximately 2–3 weeks (14). Over the lifespan of the fly, the gut epithelium is exchanged upwards of four times in females and twice in males. The steady replacement of dying ECs emphasizes the need for intrinsic developmental mechanisms that maintain intestinal integrity and function (14). Several ISC intrinsic signaling pathways have been implicated in the maintenance of ISC homeostasis under unstressed conditions, including the insulin receptor, EGFR, and Yorkie/Warts pathway (19, 20, 22–25). Basal activity of these receptor tyrosine kinase pathways are essential for the steady state turnover of ISCs, although extrinsic cues feed into these pathways to enhance ISC proliferation in response to infection or damage (18, 23, 26, 27). In this manner, EGFR signals bridge extrinsic and intrinsic cues to regulate gut tissue homeostasis in response to local and systemic conditions (17, 22).

Recent evidence suggests that an additional *Drosophila* receptor tyrosine kinase, the PDGF and VEGF receptor-related

(Pvr) protein plays a role in the control of posterior midgut physiology (28). Pvr is engaged by PDGF- and VEGF-related factors (Pvfs) 1, 2, and 3 to initiate intracellular cascades that instruct cellular activities such as negative regulation of innate immune responses, cell migration, embryonic hemocyte development, and epithelial closure (29–38). In the *Drosophila* gut, Pvr is associated with age-related and oxidative stress-related changes in the posterior midgut (28, 39). Despite these studies, it is not known whether Pvf/Pvr signals in ISCs are required for maintenance of ISC homeostasis throughout adulthood. In addition to oxidative stress and aging, other studies implicate Pvr in intestinal immune responses. For example, microarray analysis of infected *Drosophila* guts showed an increase in the expression of *pvf1* and *pvf2* (21). In our own studies, we identified the Pvr pathway as a negative regulator of immune-induced dJNK activation (38). We found that infection-induced dJNK activity enhanced the expression of *pvf2* and *pvf3*, which act in a negative feedback loop to suppress innate immune responses (38). Given the connections between infection and proliferation in the intestine, we asked whether Pvr is involved in intrinsic or extrinsic control of intestinal homeostasis.

Through the course of our investigations, we found that Pvf/Pvr signals are essential for homeostatic control of ISC proliferation and fate specification in the posterior midgut. Our studies revealed that Pvr signals in ISCs are governed through autocrine production of Pvfs. Additionally, we found that extrinsic stresses override hypoplastic defects caused by Pvf/Pvr deficiency in ISCs. In summary, we identified the Pvf/Pvr axis as a critical intrinsic regulator of basal homeostatic mechanisms required for the steady state turnover and faithful differentiation of ISCs in the *Drosophila* posterior midgut.

EXPERIMENTAL PROCEDURES

***Drosophila* Husbandry and Fly Lines**—*Drosophila* fly stocks were maintained on standard corn meal medium (Nutri-Fly Bloomington Formulation, Genesee Scientific) at 25 °C unless otherwise stated. The following fly lines were used in this study: *esg-gal4,tub-Gal80^{ts},uas-GFP* (4), *Dl-Gal4* (40), *Su (H)GBE-Gal4, UAS-GFP, pvf2-lacZ* (39), *UAS-pvr^{CA}* (41), *UAS-pvr^{DN}* (41), *UAS-pvf1, UAS-pvf2, GBE+Su (H)-LacZ* (42), *pvr⁵³⁶³* (43), *pvf2-3^A, y,w,hs-flp,UAS-mCD8:GFP; FRT* (40A), *tub-gal80, FRT* (40A); *tub-gal4, UAS-bsk^{DN}* (44), and *UAS-hep^{CA}* (44). Transgenes were expressed in ISC/EBs under the temperature-sensitive control of the *esg^{ts}* expression system as described previously (4). Briefly, the flies were raised under standard conditions (25 °C) until 3–5 days after eclosion and then shifted to 29 °C to induce transgene expression for 10 days, unless otherwise stated.

Gut Immunofluorescence—The adult flies were anesthetized with CO₂, submerged in 95% ethanol, and transferred to PBS for dissection. Isolated guts were fixed for 20 min at room temperature in fixative solution (4% formaldehyde, PBS). The guts were rinsed once in PBS and blocked overnight in PBSTBN (PBS, 0.05% Tween 20, 5% bovine serum albumin, and 1% normal goat serum) at 4 °C. The guts were stained for 3 h at room temperature in PBSTBN with a combination of the following primary antibodies: mouse anti-Delta (1:100; DSHB, C594.9B), mouse anti-armadillo (1:100; DSHB, N2 7A1), mouse anti-

prospero (1:100; DSHB, MR1A), rat anti-Pvr (1:100 (41)), rabbit anti-PDM1 (1:2000, Xiaohang Yang), mouse anti- β -gal (1:500; Sigma, G8021), or rabbit anti- β -gal (1:2000; MP Biosciences, 08559761). The guts were then washed in PBSTB (PBS, 0.05% Tween 20, 5% BSA) and stained for 1 h at room temperature in PBSTBN with Hoechst (1:1000; Molecular Probes, 33258) and with the appropriate secondary antibodies: goat anti-mouse Alexa Fluor 647 (Molecular Probes A21235), goat anti-rabbit Alexa Fluor 568 (1:1000; Molecular Probes, A11011), goat anti-rabbit Alexa Fluor 647 (Molecular Probes, A21244), or donkey anti-rat Cy3 (1:1000; Jackson ImmunoResearch, 712-165-153). The guts were washed with PBSTB and rinsed in PBS prior to visualization.

Confocal Microscopy—The guts were mounted on slides in Fluoromount (Sigma, F4680) and visualized with a spinning disk confocal microscope (Quorum WaveFX, Quorum Technologies Inc.). All gut images were collected as a Z-series and processed with Fiji software to generate a single Z-stacked image. Colocalization between individual color channels was determined using Imaris software (Bitplane Inc.) colocalization algorithms. Images were processed in Photoshop CS5 (Adobe), and figures were prepared with Illustrator CS5 (Adobe).

Statistical Analysis—GFP positive cells in posterior midguts were counted relative to the total cell population stained with Hoechst in each image with the Imaris software spot counter algorithm. To determine statistical significance, we performed a two-tailed Student's *t* test with two samples of equal variance relative to control values. *p* values of less than 0.01 are indicated with two asterisks in the figures.

Mosaic Analysis with a Repressible Cell Marker (MARCM)—*pvf2-3* flies were generated by targeted excisions of the intervening genomic region between *P{XP}Pvf2^{d00645}* and *PBac{WH}Pvf3⁰⁴⁸⁴²* (Exelixis) transposable-elements by standard genetic techniques (45). *pvr⁵³⁶³* and *pvf2-3* mutant alleles were recombined onto a *neoFRT* (40A) containing chromosome to generate *y,w,hs-flp,UAS-mCD8:GFP;pvr⁵³⁶³,neoFRT* (40A)/*Cy* and *y,w,hs-flp,UAS-mCD8:GFP;pvf2-3,neoFRT* (40A)/*Cy* flies. Recombinant flies were confirmed with PCR and complementation assays. *pvr⁵³⁶³* and *pvf2-3* recombinants were crossed with *tub-gal80,neoFRT* (40A); *tub-gal4* flies and MARCM clones were generated in the progeny by standard techniques (46). Briefly, 3–5-day-old adult flies were heat shocked at 37 °C for 2 h to induce flp recombination, and GFP positive clones were visualized after 2 weeks at 25 °C by confocal microscopy.

Infection—The flies were collected 3–5 days after eclosure, and transgenes were induced with *esg^{ts}* at 29 °C for 10 days. The flies were starved for 2 h and then fed a high dose 100 OD₆₀₀ (survival curve) or a low dose 5A₆₀₀ (MARCM) of *P. entomophila* in sucrose solution (5% sucrose and 0.5× PBS). The flies were fed the high dose of *P. entomophila* for 16 h at 29 °C and transferred to fresh food vials where the number of surviving flies were counted over time. For MARCM infection studies, the flies were heat shocked at 37 °C for 2 h to induce flp recombination and recovered at 25 °C for 16 h prior to oral infection with low dose of *P. entomophila* for 4 h at 25 °C. The flies were transferred to fresh food vials for 3 days at 25 °C prior to dissection.

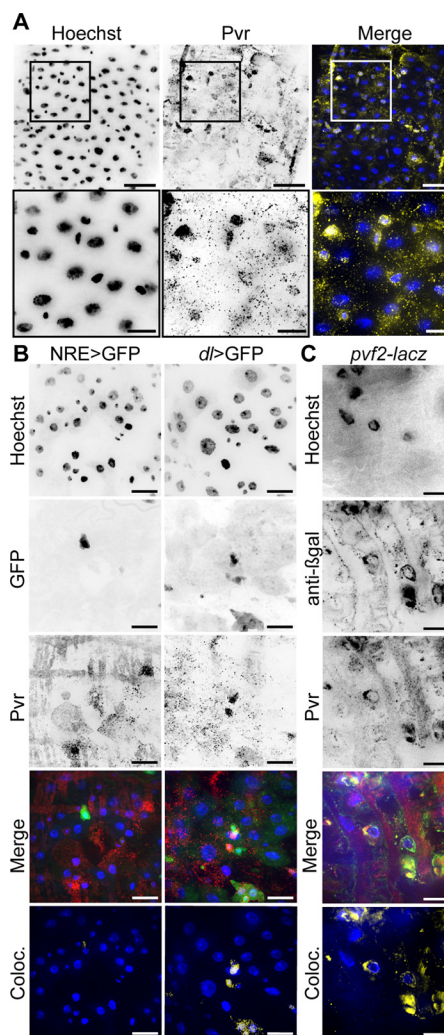


FIGURE 1. Pvr is expressed in posterior midgut ISCs. *A*, wild-type midguts were stained with Hoechst (first column) and anti-Pvr antibodies (second column). Hoechst (blue) and anti-Pvr (yellow) channels were false colored and merged in the third column. The box in the low magnification image (top row) represents the area visualized in the high magnification image (bottom row). The scale bars represent 25 and 10 μ m for low and high magnifications, respectively. *B*, Pvr localization in adult midguts that express cell type-specific GFP reporters. GFP (second row) was visualized in EBs (first column) or ISCs (second column). The midguts were stained with Hoechst (first row) and anti-Pvr antibody (third row). Hoechst (blue), GFP (green), and Pvr (red) channels were false colored and merged in the fourth row. Pixels where GFP and Pvr signals overlap were false colored (yellow) and merged with Hoechst (blue) (fifth row). The scale bars represent 15 μ m. *C*, Pvr and the *pvf2-lacZ* reporter colocalize (Coloc.) in posterior midgut ISCs. Guts were isolated from *pvf2-lacZ* flies and stained with Hoechst (first panel), anti- β -gal (second panel), and anti-Pvr antibodies (third panel). Hoechst (blue), anti- β -gal (green), and Pvr (red) channels were false colored and merged in the fourth panel. Pixels where *pvf2*-reporter (β -gal) and Pvr signals overlap were false colored (yellow) and merged with Hoechst (blue) (fifth panel). The scale bars represent 10 μ m.

RESULTS

Posterior Midgut ISC Express Pvr and Pvf2—To determine whether Pvr is expressed in the posterior midgut, we stained posterior midguts from 3–5-day-old adult wild-type *Drosophila* with an anti-Pvr antibody (Fig. 1A). Pvr antibodies marked a subpopulation of cells with relatively small nuclei reminiscent of the ISC/EB cell population and distinct from the larger polyploid nuclei found in ECs. To determine the precise identity of the Pvr positive cell population, we visualized Pvr in the midguts of adult flies that express cell type-specific GFP report-

Pvr Regulates Drosophila Midgut Homeostasis

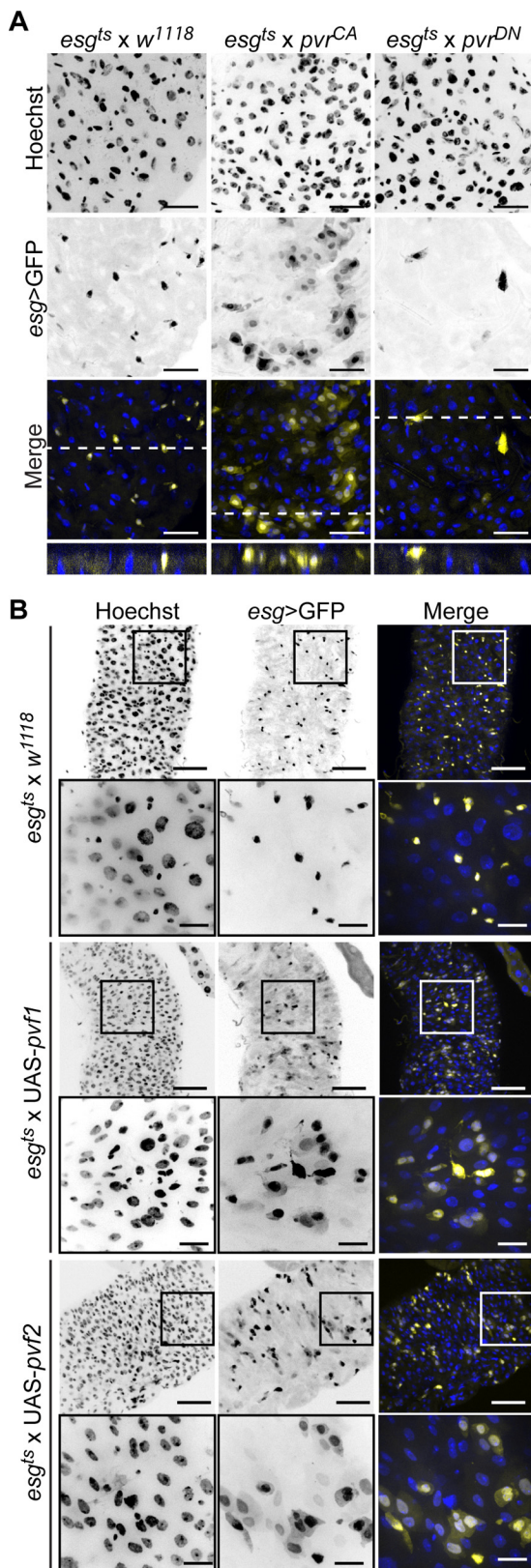


FIGURE 2. Pvr is required for intestinal homeostasis. *A*, immunofluorescence microscopy of posterior midguts upon expression of Pvr^{CA} (*second column*) and Pvr^{DN} (*third column*) in ISC/EBs relative to control midguts (*first column*). The guts were stained with Hoechst (*first row*), and ISC/EBs were visualized by GFP expression (*second row*). Hoechst (blue) and GFP (yellow) channels were false colored and merged (*third row*). The white dashed line represents the area shown in cross-section in *fourth row*. The scale bars represent 25 μm . *B*, visualization of posterior midgut morphology upon UAS-*pvf2*

ers. We used a Notch reporter element (NRE)-GAL4 driver line and a Delta-Gal4 driver line to express GFP in EBs (NRE > GFP⁺) and ISCs (*dl* > GFP⁺), respectively. We then performed colocalization analysis on GFP and anti-Pvr fluorescence in the respective stains to assess the degree of overlap between cell type-specific markers and Pvr (Fig. 1*B*). We found a marked colocalization of Pvr with *dl* > GFP positive ISCs and essentially no overlap with EBs (NRE > GFP).

Previous studies with a *pvf2-lacZ* reporter fly line that expresses β -gal under control of the *pvf2* promoter uncovered Pvf2 expression in midgut ISCs (28). To determine whether Pvr and Pvf2 expression overlap, we stained posterior midgut ISCs from *pvf2-lacZ* flies with anti-Pvr and anti- β -gal antibodies (Fig. 1*C*). In these studies, we observed a strong overlap between Pvr and Pvf2 in individual cells in the posterior midgut. Thus, we conclude that posterior midgut ISCs coexpress Pvr and Pvf2.

The Pvr Axis Controls Midgut Homeostasis—Because posterior midgut ISCs coexpress Pvr and a *pvf2-lacZ* reporter, we monitored the impact of Pvr signals on gut homeostasis. To accomplish this, we specifically hyperactivated or inhibited Pvr signals in ISCs with the targeted expression of constitutively active Pvr (Pvr^{CA}) and dominant negative Pvr (Pvr^{DN}) transgenes, respectively. We expressed transgenes in ISC/EBs under the control of the *esg^{ts}* (*esg-GAL4*, *UAS-GFP*, *tub-GAL80^{ts}*) TARGET system (4, 47). In this line, the *esg* promoter-driven GAL4 expression is blocked by a temperature-sensitive mutant allele of *GAL80* (*GAL80^{ts}*) at permissive temperatures (<25 °C) but not at restrictive temperatures (>29 °C). This system allows us to prevent *esg*-mediated transgene expression from embryogenesis through pupariation and restrict transgene expression to adult stages.

We reared flies at the restrictive temperature, until 3–5 days of adulthood and then shifted flies to 29 °C to drive Pvr^{CA} or Pvr^{DN} expression in ISC/EB cells for 10 days (Fig. 2*A*). Control *esg* > GFP positive cells display a typical ISC/EB partnership of small, evenly spaced and frequently paired cells. Cross-sections revealed that wild-type *esg* > GFP positive cells were typically in close association with the basal lamina as expected for progenitor cells. In stark contrast, Pvr^{CA} activation resulted in a striking expansion of *esg^{ts}* > GFP positive cell clusters with distinctly altered cellular morphology. Pvr^{CA} promoted the expression of *esg* > GFP in an increased number of small cells and larger polyploid cells reminiscent of the ISC/EB and EC cell populations, respectively. Analysis of cross-sections from Pvr^{CA} midguts revealed that *esg^{ts}* > GFP positive cells extended through the gut epithelium from the basal lamina to the intestinal lumen. In striking contrast, Pvr inhibition through the expression of Pvr^{DN} resulted in considerably fewer *esg* > GFP positive cells that were rarely paired. In midgut cross-sections,

(*third and fourth rows*) and UAS-*pvf2* (*fifth and sixth rows*) expression in ISC/EBs relative to control midguts (*first and second rows*). The guts were stained with Hoechst (*first column*), and ISC/EBs were visualized by GFP expression (*second column*). Hoechst (blue) and GFP (yellow) channels were false colored and merged in the *third column*. The boxed areas in the low magnification *first, third, and fifth rows* indicate the areas shown in high magnification in the *second, fourth, and sixth rows*, respectively. The scale bars represent 50 and 15 μm for low and high magnification images, respectively.

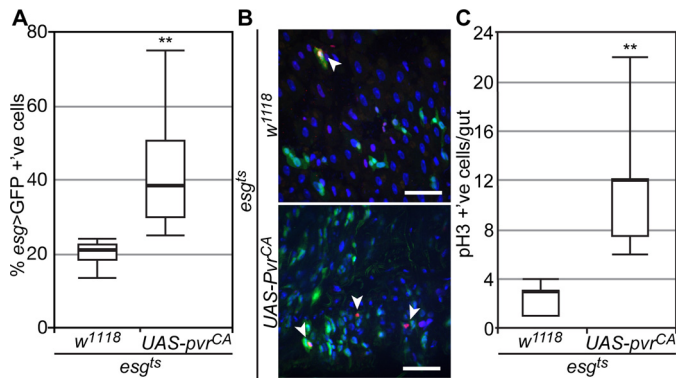


FIGURE 3. Pvr activity promotes intestinal mitosis. *A*, quantification of GFP positive cells in posterior midguts upon expression of Pvr^{CA} ($n = 10$) under the control of *esg^{ts}*, relative to control guts as indicated ($n = 10$). All cells were stained with Hoechst, and GFP positive cells were calculated as a percentage of total cells per field. *B*, representative immunofluorescence image of posterior midguts upon expression of Pvr^{CA} (bottom panel) in ISCs/EBs relative to control midguts (top panel). The guts were stained with Hoechst and anti-pH3, and ISC/EBs were visualized by GFP expression. Hoechst (blue), pH3 (red), and GFP (green) channels were false colored and merged. Arrowheads point to pH3 positive cells. The scale bars represent 25 μm . *C*, quantification of pH3 positive cells in whole guts upon expression of Pvr^{CA} ($n = 12$) under the control of *esg^{ts}*, relative to control guts as indicated ($n = 14$). All of the cells were stained with Hoechst and anti-pH3, and the number of pH3 positive cells was calculated per gut. In *A* and *C*, box plots show the median number of GFP and pH3 positive cells (thick line) respectively, flanked by the first quartile (bottom edge) and third quartile values (top edge), whereas the top and bottom whiskers indicate the highest and lowest data points for each data set, respectively. **, $p < 0.01$.

these *esg* > GFP cells were strictly associated with the basal lamina.

These observations prompted us to explore the impact of Pvf ligand expression on the posterior midgut. For these studies, we expressed Pvf1 and Pvf2 in adult gut ISC/EBs with *esg^{ts}*, as described above (Fig. 2*B*). As anticipated, wild-type *esg^{ts}* > GFP positive cells appear small, often paired, and evenly distributed throughout the posterior midgut. In contrast, *esg^{ts}*-mediated expression of Pvf1 or Pvf2 greatly amplified *esg^{ts}* > GFP positive cell numbers with approximately half of all cells staining positive for GFP. High magnification images showed clear changes in the morphology of *esg^{ts}* > Pvf1 and *esg^{ts}* > Pvf2 midgut cells, relative to control midgut cell. As with Pvr^{CA}, expression of either Pvf1 and Pvf2 promotes the expansion of *esg^{ts}* > GFP positive cell clusters composed of both large and small nucleated cells reminiscent of EC and ISC/EB cell populations, respectively. Combined, these data suggest that Pvr signals regulate midgut homeostasis.

Pvr Promotes Intestinal Hyperproliferation—Our initial tests established that Pvr^{CA} drives the expansion of *esg^{ts}* > GFP positive cells in posterior midguts. To quantify the extent of this expansion, we calculated the percentage of *esg^{ts}* > GFP positive cells in midguts that expressed Pvr^{CA}, relative to control midguts (Fig. 3*A*). In line with previous studies, we found that 21% of all cells in the posterior midgut of wild-type *esg^{ts}* > GFP flies were GFP positive. Pvr^{CA} expression in ISCs/EBs doubled the average percentage of *esg^{ts}* > GFP positive cells (42% *esg^{ts}* > GFP +ve) in the posterior midgut. To determine whether increased ISC divisions were responsible for greater *esg^{ts}* > GFP cell numbers, we visualized ISC mitosis with an anti-phospho-H3 (pH3) antibody (Fig. 3*B*). We found that Pvr^{CA} expres-

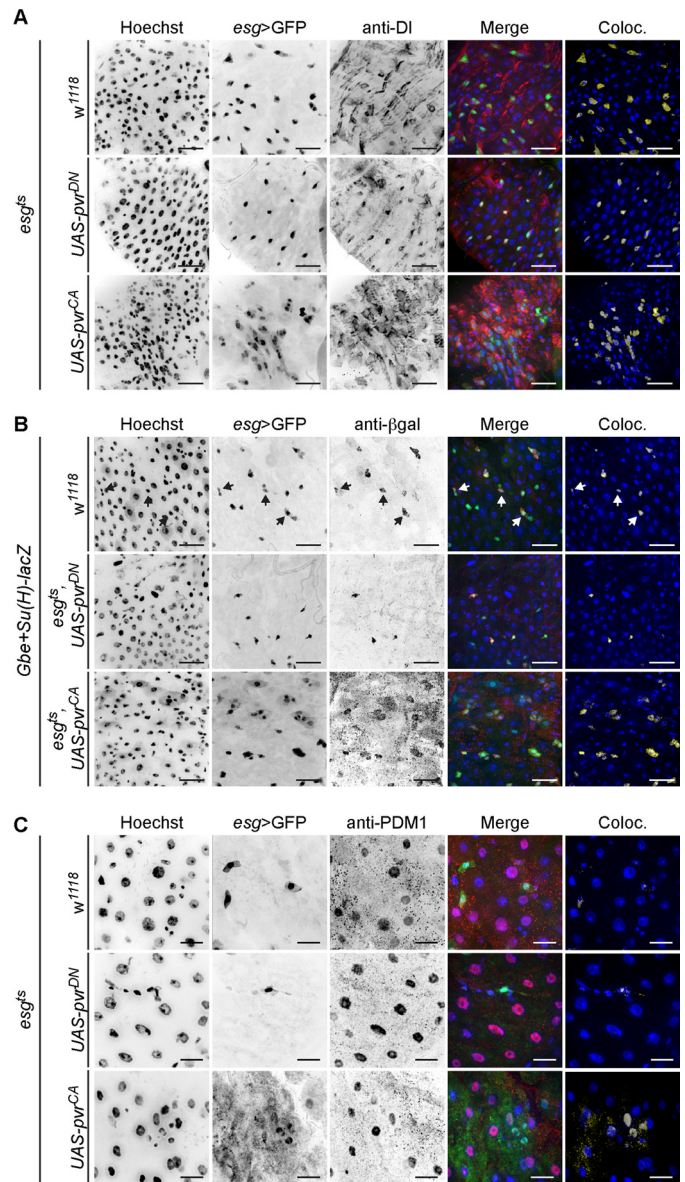


FIGURE 4. Pvr controls midgut cell development. In all panels, posterior midguts were visualized upon *pvr^{DN}* (second row) or *pvr^{CA}* (third row) transgene expression under the control of *esg^{ts}*, relative to control midguts (first row). The guts were stained with anti-Dl (*A*), anti- β -gal (*B*), or anti-PDM1 (*C*) antibodies to mark ISCs, EBs, and ECs, respectively. All of the cells were stained with Hoechst (first column), and *esg^{ts}* positive cells were visualized with GFP fluorescence (second column). Hoechst (blue), GFP (green), and cell type-specific (red) channels were false colored and merged in the fourth row. Pixels where GFP and cell type-specific marker signals overlap were false colored (yellow) and merged with Hoechst (blue) (fifth row). Arrows indicate EBs within ISC/EB equivalence groups. The scale bars represent 25 μm (*A* and *B*) and 15 μm (*C*). Coloc., colocalization.

sion in ISCs/EBs significantly enhanced the number of mitotic cells in the *Drosophila* gut (Fig. 3*C*).

Pvr Signals in ISCs Are Essential for the Appropriate Development of Intestinal Cells—Our preliminary observations hint at a possible requirement for Pvr signals in intestinal homeostasis. To explore this possibility further, we determined the identity of individual midgut cells in *esg^{ts}* flies that express Pvr^{CA} or Pvr^{DN}. For these experiments, we used anti-Dl antibodies, anti-PDM1 antibodies, and Notch reporter element (NRE-lacZ) transgenic flies to mark ISCs, ECs, and EBs (Fig. 4), respectively.

Pvr Regulates Drosophila Midgut Homeostasis

As expected, we observed the archetypal DI/Notch equivalence group in wild-type guts. *esg^{ts}* > GFP positive cells were most often DI positive ISCs, and when *esg^{ts}* > GFP positive cells were paired, the partnership was completed with a NRE > lacZ positive EB cell, as indicated with arrows in Fig. 4B. Further examination of *esg^{ts}* > GFP positive cells showed no overlap with the EC marker anti-PDM1 (Fig. 4C).

Our observations on wild-type midguts are in stark contrast to the observed distribution of ISC, EB, and EC specific markers with *esg^{ts}*-mediated expression of Pvr^{CA}. Hyperactivation of Pvr signals expanded the *esg^{ts}* > GFP population with a corresponding increase in the coexpression of ISC, EB, and EC cell type-specific markers in midguts. Specifically, we found that Pvr^{CA} increased the total number of DI positive ISCs, whereas a significant population of *esg^{ts}* > GFP positive cells were DI negative (Fig. 4A). Additionally, we found that Pvr activation increased the number of EBs within *esg* > GFP positive cell clusters (Fig. 4B). These EB cells were frequently observed in close proximity to other EBs and non-EB *esg^{ts}* > GFP positive cells. Finally, we observed a strong overlap of PDM1 and *esg^{ts}* > GFP upon Pvr^{CA} expression. These data demonstrate that hyperactive Pvr signals disrupts midgut homeostasis and promote intestinal dysplasia (Fig. 4C).

In contrast, expression of the Pvr^{DN} transgenes with *esg^{ts}* resulted in a marked reduction of *esg^{ts}* > GFP positive cells, relative to control guts. Furthermore, suppression of Pvr signals greatly diminished the number of GFP positive paired cells with a strong bias toward maintenance of DI positive ISCs within the *esg^{ts}* > GFP populations (Fig. 4A). These data indicate that Pvr signals are required for cells to progress beyond the ISC fate and establish the ISC/EB equivalence group.

Autocrine Pvr Signals Regulate ISC Fate Determination—To directly test a requirement for Pvr in the homeostatic control of ISC development, we examined the midgut architecture of *pvr* and *pvf* mutant flies. A gene duplication event generated the *pvf2* and *pvf3* genes in a tandem genomic arrangement and hints at overlapping and potentially redundant functions among the two ligands. This prompted us to generate a genomic deletion that specifically ablates *pvf2* and *pvf3* (*pvf2-3Δ*, hereafter abbreviated as *pvf2-3*; supplemental Fig. S1). Consistent with redundant developmental requirements for *pvf2* and *pvf3*, the *pvf2-3* deletion was homozygous lethal and phenotypically similar to *pvr⁵³⁶³* null mutant embryos, whereas the single mutant flies were homozygous viable. Because both *pvr⁵³⁶³* and *pvf2-3* mutations are homozygous lethal, we generated homozygous mutant ISC clones in otherwise heterozygous guts through mitotic recombination using the MARCM technique (46). Homozygous control or mutant clones were marked with the expression of membrane bound GFP (Fig. 5A). As expected, wild-type clones contain large numbers of cells with mixed cellular morphology that primarily consist of large ECs derived from ISC proliferation and differentiation. In contrast, we observed a dramatic collapse in cell numbers in clones mutant for *pvr* or *pvf2-3*. Both *pvr⁵³⁶³* and *pvf2-3* clones were severely handicapped in their proliferative potential and appeared significantly smaller (1–3 cells/clone) than their wild-type counterparts (>10 cells/clone) (Fig. 5B). Furthermore, the ISC developmental program in *pvr⁵³⁶³* and *pvf2-3* mutant cells

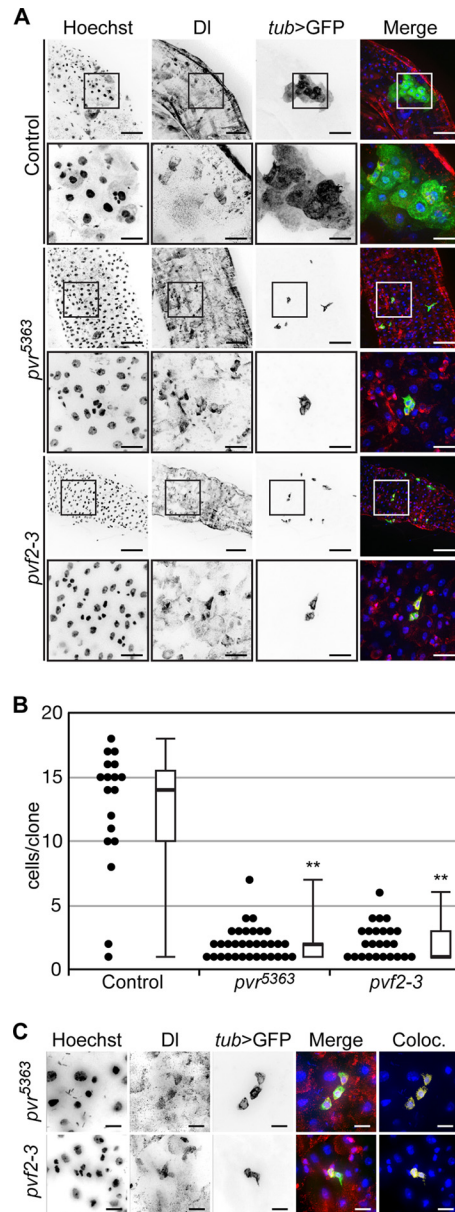


FIGURE 5. Autocrine Pvr/Pvf signals in ISCs establish mature midgut cells.

A, *pvr⁵³⁶³* (third and fourth rows) and *pvf2-3* (fifth and sixth rows) MARCM clones in the posterior midgut compared with wild-type control midguts (first and second rows). The guts were stained with Hoechst (first column) and anti-DI antibodies (second column). MARCM clones were visualized by *tub* > GFP expression in the third row. Hoechst (blue), DI (red), and *tub* > GFP (green) channels were false colored and merged in the fourth column. The boxed areas in the low magnification first, third, and fifth rows indicate the areas shown in high magnification in the second, fourth, and sixth rows, respectively. The scale bars represent 50 and 15 μ m for low and high magnifications, respectively. **B**, quantification of GFP positive cells in *pvr⁵³⁶³* and *pvf2-3* MARCM clones compared with control clones. Black circles represent individual data points. Box plots show the median number of cells/clone (thick line) flanked by the first (bottom edge) and third quartile (top edge) values, whereas the whiskers represent peripheral values in each data set. **, $p > 0.01$. **C**, high magnification images of *pvr⁵³⁶³* (first rows) and *pvf2-3* (second row) MARCM clones. The guts were stained with Hoechst (first column) and anti-DI antibodies (second column). MARCM clones were visualized by *tub* > GFP expression (third column). Hoechst (blue), DI (red), and *tub* > GFP (green) channels were false colored and merged in the fourth row. The scale bars represent 10 μ m.

appeared completely disrupted because we found no large polyploid ECs within the clones.

Consistent with an essential requirement for the Pvr pathway in homeostatic intestinal development, we found that all

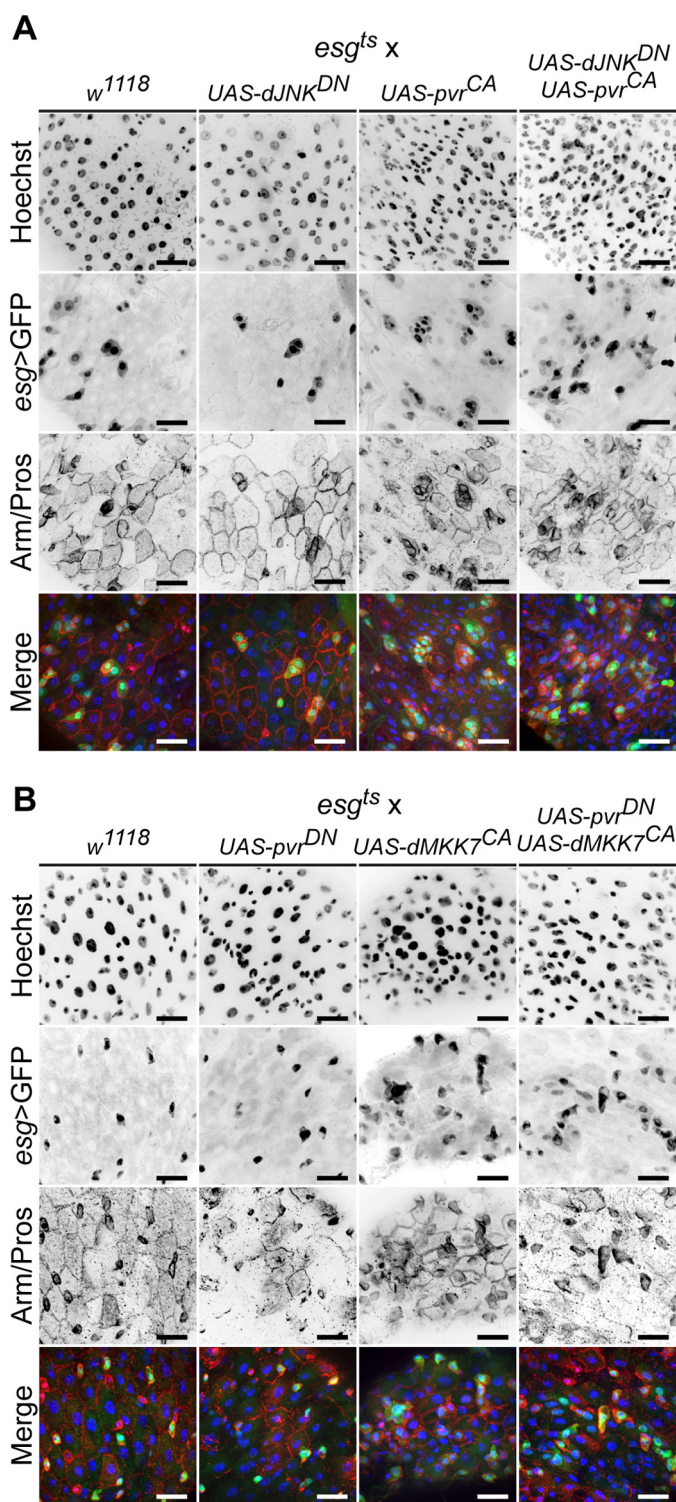


FIGURE 6. Pvr regulates ISC homeostasis independent of extrinsic dJNK cues. *A*, *dJNK*^{DN} (second column) and *pvr*^{CA} (third column) transgenes were expressed individually or together (fourth column) in ISC/EBs, and posterior midgut morphology was visualized relative to control midguts (first column). The guts were stained with Hoechst (first row), and anti-Arm/Pros antibodies (third row), whereas ISC/EBs were visualized with *esg*^{ts} > GFP expression (second row). Hoechst (blue), GFP (green), and anti-Arm/Pros channels (red) channels were false colored and merged in the fourth row. The scale bars represent 25 μm. *B*, *pvr*^{DN} (second column) and *dMMK7*^{CA} (third column) transgenes were expressed individually or together (fourth column) by *esg*^{ts}, and posterior midgut morphology was visualized relative to control midguts (first column). The guts were stained with Hoechst (first row) and anti-Pros/Arm antibodies (third row), whereas ISC/EBs were visualized with *esg*^{ts} > GFP (second row).

*pvr*⁵³⁶³ and *pvf2-3* mutant clones are comprised entirely of Df positive ISCs (Fig. 5C). These data establish that signals through the Pvf/Pvr axis are essential for ISCs to progress along their developmental program to generate mature cell types in the posterior midgut. Interestingly, proximal Pvf production by surrounding heterozygous cells fails to compensate for the loss of Pvf2 and Pvf3 in *pvf2-3* mutant clones. These findings suggest that Pvf is produced and sensed by individual ISCs in an autocrine fashion to regulate Pvr-mediated homeostatic signals. In summary, our findings establish that Pvf/Pvr intrinsic signals are essential for ISC homeostatic proliferation and differentiation and that loss of Pvr leads to midgut hypoplasia.

Pvr Acts Independently of dJNK to Control Midgut Homeostasis—We showed previously that immune-induced dJNK activation promotes *pvf2* and *pvf3* expression and that Pvr pathway activation regulates dJNK signals in a negative feedback loop (38). Because dJNK signals feed into ISC proliferative controls (14, 16, 48), we assessed the genetic relationship between Pvr and dJNK signals in ISC proliferation. To assess whether Pvr^{CA} dysplastic cues proceed through dJNK, we used *esg*^{ts} to simultaneously hyperactivate Pvr and inhibit dJNK in ISCs. As a corollary, we simultaneously inhibited the Pvr pathway and activated the dJNK pathway to determine whether dJNK-associated proliferative cues require Pvr. In the first set of experiments, we expressed Pvr^{CA} and dJNK^{DN} together or independently in 3–5-day-old adult flies for 10 days, alongside wild-type control flies (Fig. 6A). To assess midgut morphology, we stained guts with anti-Armadillo antibodies to mark cell junctions and with anti-Prospero antibodies to label EEs. We then visualized ISC/EBs by *esg*^{ts} > GFP fluorescence. Consistent with our previous findings, Pvr^{CA} expression drives the expansion of *esg*^{ts} > GFP positive cells in the posterior midgut. In contrast, inhibition of dJNK signals with dJNK^{DN}, mildly reduced total *esg*^{ts} > GFP positive cell numbers, relative to control guts. Simultaneous *esg*^{ts}-mediated expression of Pvr^{CA} and dJNK^{DN} phenocopied the proliferation of *esg*^{ts} > GFP positive cells observed with Pvr^{CA} expression alone. From these data we conclude that Pvr^{CA} signals promote the expansion of *esg*^{ts} > GFP positive cells in the posterior midgut independently of dJNK activity.

To determine whether dJNK-induced ISC proliferation is the outcome of downstream Pvr pathway activation, we used the *esg*^{ts} driver system to express dMMK7^{CA}. dMMK7^{CA} is a constitutively active MAPKK that engages dJNK. We coexpressed dMMK7^{CA} and Pvr^{DN} with *esg*^{ts} to simultaneously promote dJNK activity while blocking the Pvr pathway in ISC/EBs, respectively (Fig. 6B). We also individually expressed dMMK7^{CA} and Pvr^{DN} with *esg*^{ts}, alongside wild-type flies, as controls. Hyperactive dJNK activity in ISCs rapidly induces gut hyperplasia and eventually kills the affected fly; therefore dMMK7^{CA} expression was limited to 3 days in all flies. In agreement with previous studies, constitutive dJNK activation induced profound changes in the number and morphology of *esg*^{ts} > GFP positive cells, relative to control midguts. However, when dMMK7^{CA} and Pvr^{DN} are coexpressed with *esg*^{ts}, the pro-

Hoechst (blue), GFP (green), and anti-Arm/Pros channels (red) channels were false colored and merged in the fourth row. The scale bars represent 25 μm.

Pvr Regulates Drosophila Midgut Homeostasis

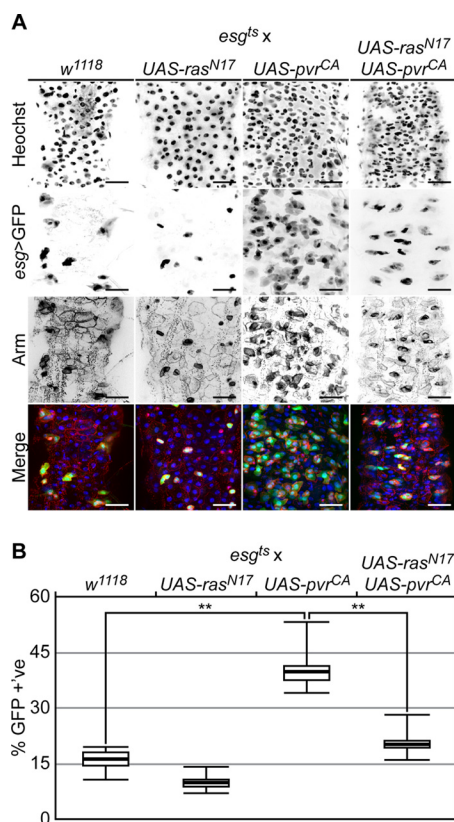


FIGURE 7. Pvr acts through Ras to control ISC homeostasis. *A*, *ras^{N17}* (second column), and *pvr^{CA}* (third column) transgenes were expressed individually or together (fourth column) by *esg^{ts}* and posterior midgut morphology was visualized relative to control midguts (first column). The guts were stained with Hoechst (first row) and anti-Arm antibodies (third row), whereas ISC/EBs were visualized with *esg^{ts}* > GFP expression (second row). Hoechst (blue), GFP (green), and anti-Arm (red) channels were false colored and merged in the fourth row. The scale bars represent 25 μ m. *B*, quantification of GFP positive cells in *A*. The percentages of GFP positive cells were calculated in posterior midguts that expressed *Pvr^{CA}* ($n = 5$), *Ras^{N17}* ($n = 8$), or *Pvr^{CA}* and *Ras^{N17}* together ($n = 8$) with *esg^{ts}*, relative to controls ($n = 6$). The box plots show the median percentage of GFP positive cells (thick line), flanked by the first quartile (bottom edge) and third quartile values (top edge), whereas the top and bottom whiskers indicate the highest and lowest data points for each data set, respectively. **, $p < 0.01$.

liferative signals generated through constitutive dJNK activation overwhelm any suppressive effects of *Pvr^{DN}*. We conclude that *Pvr* and dJNK pathways act independently to regulate ISC proliferation in the posterior midgut. However, we cannot exclude the possibility that *Pvr* and dJNK pathways promote ISC proliferation through shared downstream effectors.

Ras Activity Is Required for Pvr-induced Intestinal Dysplasia—Previous studies showed that constitutive Ras activity in ISCs promotes hyperproliferation and posterior midgut dysplasia (25). Given our data that hyperactive *Pvr* dysplastic cues are independent of the dJNK pathway, we asked whether *Pvr* intracellular signals proceed through the Ras pathway. To assess the downstream requirement for Ras in *Pvr* controls of intestinal homeostasis, we simultaneously expressed *Pvr^{CA}* with a dominant negative Ras variant (*Ras^{N17}*). For these experiments, we expressed *Pvr^{CA}* and *Ras^{N17}* transgenes together or independently in 3–5-day-old adult flies for 10 days, alongside wild-type control flies (Fig. 7A). We monitored posterior midgut morphology with anti-Armadillo antibody stain, ISC/EBs with *esg* > GFP, and the total intestinal cell population with

Hoechst fluorescence. We then quantified ISC/EBs with *esg* > GFP and total cell populations with Hoechst in each field, and we calculated the percentage of *esg* > GFP positive cells (Fig. 7B). Consistent with our previous findings, *Pvr^{CA}* expression promoted cellular dysplasia and significantly increased the percentage of *esg* > GFP positive cells relative to wild-type controls in posterior midguts. Expression of *Ras^{N17}* alone with *esg^{ts}* had a mild reducing effect on ISC/EB cell numbers. Furthermore, we found that coexpression of *Ras^{N17}* and *Pvr^{CA}* significantly abrogated the *Pvr^{CA}* dysplastic phenotype. These findings indicate that Ras is a downstream signaling component in the *Pvr*-dependent regulation of intestinal homeostasis.

Extrinsic Proliferative Cues Override Intrinsic Roles of Pvr in Intestinal Homeostasis—Our data established that the dJNK proliferative signals overwhelm the *Pvr^{DN}* phenotype in posterior midgut ISCs. Because dJNK activates ISC proliferation in response to acute stress such as microbial challenge, we asked whether oral infection-induced ISC proliferation could also override the hypoplastic phenotypes of *pvr⁵³⁶³* and *pvf2-3*. Oral infection of adult *Drosophila* with low concentrations of the enteropathogenic bacterium *P. entomophila* promotes the rapid proliferation and differentiation of ISCs to replenish damaged ECs and maintain posterior midgut epithelial continuity (16, 49). We therefore tested whether *P. entomophila* oral-infection induces expansion of *pvr⁵³⁶³* and *pvf2-3* mutant clones in the posterior midgut. We generated GFP-marked wild-type, *pvr⁵³⁶³*, and *pvf2-3* clones and fed adult flies low concentrations of *P. entomophila* in sucrose or sucrose alone, as a control (Fig. 8A). In uninfected guts wild-type, *pvr⁵³⁶³*, and *pvf2-3* clones were small, sparsely distributed, and mostly single cells after 3 days. This reflects the generally low homeostatic proliferation rate of ISCs in the absence of challenge. As expected, *P. entomophila* infection increased the size and cellular architecture of GFP-marked wild-type clones, with an anticipated expansion of large polyploid ECs that account for the majority of cells within the clone. These data overlap with previous reports that ISCs rapidly proliferate and differentiate into mature cell types to maintain tissue homeostasis upon *P. entomophila* infection. Strikingly, *pvr⁵³⁶³* and *pvf2-3* mutant clones were indistinguishable from wild-type clones. In each case, we observed a clear expansion of GFP positive clones that primarily consist of large ECs derived from ISC proliferation and differentiation. We conclude that extrinsic stress-induced proliferative signals override the hypoplastic defects in ISCs attributed to the loss of intrinsic *Pvf/Pvr* signals upon intestinal infection.

Because *Pvr* dampens innate immune responses (38) and epithelial renewal programs remain intact in the midgut of infected *pvr* mutants, we reasoned that a loss of *Pvr* pathway activity may enhance host responses to bacterial challenge. To determine whether *Pvr* signals impact survival rates after oral infection with a lethal dose of *P. entomophila* (15), we expressed *Pvr^{CA}* and *Pvr^{DN}* transgenes in ISC/EBs of 3–5-day-old adult flies for 10 days. We then orally infected flies with *P. entomophila* and counted the number of surviving flies over time (Fig. 8B). We found that wild-type and *esg^{ts}* > *Pvr^{CA}* flies rapidly succumbed after *P. entomophila* oral infection. Remarkably, inhibition of *Pvr* signals with *esg^{ts}*-mediated expression of

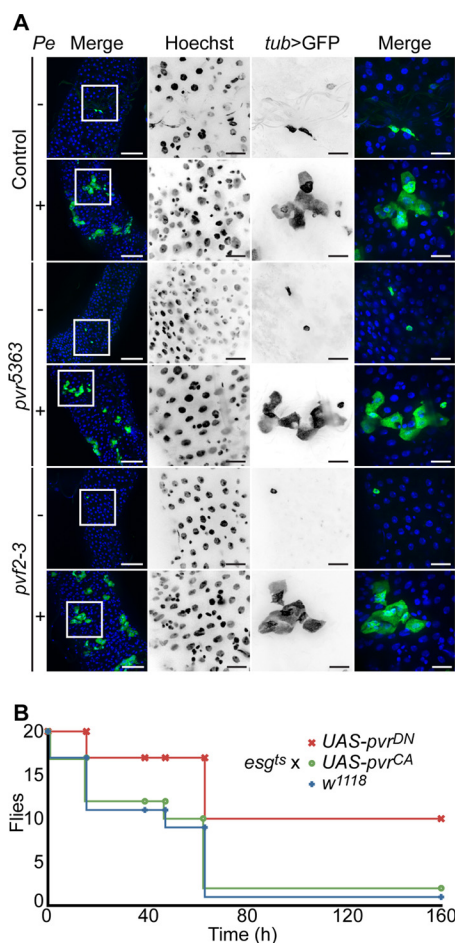


FIGURE 8. Extrinsic stress signals override Pvr intrinsic homeostatic controls. Infection-induced proliferative signals override Pvr-regulation of ISCs. *A*, wild-type (first and second rows), *pvr*⁵³⁶³ (third and fourth rows), and *pvf2-3* (fifth and sixth rows) MARCM clones in uninfected and *P. entomophila*-infected (*Pe*) adult posterior midguts as indicated. The guts were stained with Hoechst (second column), and wild-type, *pvr*⁵³⁶³, and *pvf2-3* mutant clones were visualized with *tub* > GFP in column 3. Hoechst (blue), DAPI (red), and *tub* > GFP (green) channels were false colored and merged in the first and fourth columns. The boxed areas in the low magnification first column indicate the area shown in high magnification in the second through fourth columns. The scale bars represent 50 and 15 μ m for low and high magnifications, respectively. *pvr*⁵³⁶³ and *pvf2-3* mutant clones expand in response to *P. entomophila*-infection. *B*, Pvr signals control survival to *P. entomophila* oral infection. Survival curve of adult flies that express *pvr*^{CA} or *pvr*^{DN} transgenes with *esg*^{ts} in EB/ISCs upon oral infection with *P. entomophila*, relative to control *w*¹¹¹⁸ flies. The flies were infected orally with *P. entomophila*, and the surviving flies were counted at the indicated times. Pvr inhibition enhances survival to *P. entomophila* infection.

Pvr^{DN} improved survival to *P. entomophila* infection. For example, half the wild-type and *esg*^{ts} > *Pvr*^{CA} flies succumb to infection within 64 h of infection, whereas we observed no appreciable loss of *esg*^{ts} > *Pvr*^{DN} flies. These data show that inhibition of Pvr signals enhances fly survival to oral infection with *P. entomophila*, despite the apparent requirement for Pvr in ISC proliferation under normal conditions.

DISCUSSION

The metazoan gut is under constant bombardment from environmental pressures that damage exposed epithelial cells and corrupt intestinal tissue integrity. The human intestinal tract alone is home to over 10 trillion bacteria (50), which equals ~10-fold more bacterial cells than human somatic and germ

cells combined. As a result, the intestinal microbiome may contain greater than 100 times more unique genetic sequences than are present in the entire human genome (50). This highlights the remarkably complex relationship between metazoans and their intestinal environment and the requirement for sophisticated intercellular communication networks that coordinate homeostatic responses to protect organ function from enteropathogenic challenges.

Studies of the *Drosophila* midgut model revealed that ISC homeostasis is maintained through an elaborate balance of multiple pathways that respond to extrinsic insults and intrinsic requirements for the orderly development of mature epithelial cell types (2). ISCs proliferate and differentiate rapidly in response to stress signals. However, in the absence of these signals, intrinsic cues guide low level ISC division to ensure a stable population of progenitor cells (2). Previous studies highlighted the overlapping contributions of Jak/Stat, EGFR, insulin receptor, Hippo/Wrts, and JNK pathways to meet intestinal tissue requirements. The Jak/Stat pathway is a major regulator of intestinal homeostasis in response to injury or stress with additional contributions to stem cell differentiation under unstressed conditions (14, 51). The EGFR pathway amalgamates paracrine stress responsive signals with autocrine signals to regulate ISC growth and proliferation (17, 18, 22, 25). The insulin receptor pathway is a general regulator of homeostatic proliferative controls in posterior midgut ISCs and responds to nutritional requirements and epithelial damage (23, 52–54). Along with the strong non-cell autonomous requirement for the Wrt/Hippo pathway in the generation of stress signals, there is also evidence that Wrt/Hippo plays a role in the regulation of ISC autonomous homeostatic signals (19, 20, 24, 27, 55). Finally, oxidative stress activates the dJNK pathway to guide the production of mitogenic signals that drive the rapid proliferation and differentiation of the underlying ISCs (16, 48, 56, 57).

In our studies, we uncovered a novel requirement for the Pvr/Ras signal transduction pathway in the regulation of ISC homeostatic controls in the posterior midgut. We showed that loss of the Pvr receptor in ISCs completely blocks the ISC/EB/EC developmental program. Instead, mutant cells fail to proliferate and retain their identity as DAPI positive ISCs. Because the simultaneous deletion of *pvf2* and *pvf3* exclusively from ISCs in an otherwise heterozygous background phenocopies the *pvr* mutant phenotype, we conclude that Pvf2 and Pvf3 are ISC autonomous regulators of ISC proliferation. Furthermore, these observations indicate that autocrine Pvf/Pvr signals guide ISC homeostasis. This hypothesis is entirely consistent with the observed ISC expression patterns for Pvr and Pvf2, where both ligand and receptor are restricted to ISCs. Our findings also highlight a noteworthy distinction between Pvr and previously described intrinsic regulators, because extrinsic stress cues are epistatic to Pvr in relation to proliferation. This is in contrast to the findings of EGFR and insulin receptor pathway mutants that display proliferative defects under unstressed conditions and upon enteropathogenic infection. Thus, our studies suggest that Pvr is an ISC autonomous homeostatic regulator (Fig. 9).

Age-associated decline in stem cell activity has been implicated in the development of several disease conditions such as

Pvr Regulates *Drosophila* Midgut Homeostasis

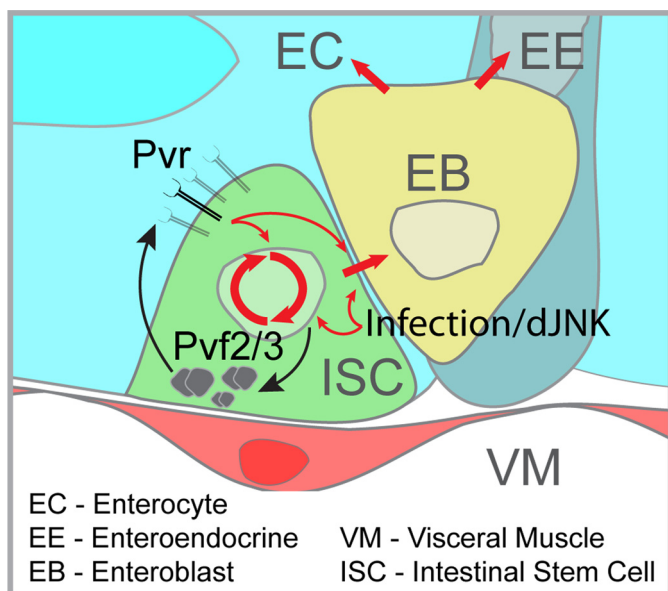


FIGURE 9. Model of Pvf/Pvr regulation of ISC homeostasis. ISC intrinsic Pvr signals are engaged by autocrine Pvf2/3 expression to maintain homeostatic proliferation and differentiation in the *Drosophila* posterior midgut. Extrinsic stress signals overwhelm Pvr controls of ISC homeostasis and independently promote compensatory proliferation and differentiation in response to enteropathogenic infection. Pvr signals are required for the steady state turnover and fate determination of ISCs under unstressed conditions.

progressive organ failure and cancer. Because intrinsic signals are responsible for the maintenance of ISC pools over the lifetime of the animal, the loss or disruption of these pathways significantly affects age-related disease progression (57). In aged *Drosophila* posterior midguts, ISCs hyperproliferate and the resultant pool of daughter cells fails to differentiate correctly, causing dysplasia and gradual degeneration of the intestinal epithelium (48). In agreement with a connection between aging and deregulated ISC homeostasis, genetic manipulation of factors that suppress ISC proliferation are associated with reduced age-related intestinal dysplasia and prolonged longevity (28, 39, 48, 57). We showed that Pvf/Pvr hyperactivity in ISCs drives intestinal dysplasia, and previous studies found that production of Pvf2 by ISCs engages the Pvr pathway to activate p38 and contributes to age-related changes in the *Drosophila* posterior midgut (28, 39). These observations support our model of Pvr as an intrinsic regulator of ISC homeostasis.

The *Drosophila* Pvr protein shares significant sequence and structural similarity with the human VEGF and PDGF families of receptor tyrosine kinases (58). In mammals, the VEGF and PDGF receptors function in multiple cellular processes that include growth, proliferation, migration, and differentiation (58). For example, studies of mice mutant in PDGF-A and PDGFR- α showed a spectrum of development defects in organogenesis (58). Of particular relevance to our studies is the finding that PDGF-A and PDGFR- α mutant mice display severe defects in gastrointestinal tract architecture predominantly in the upper small intestine (59). During organogenesis the paracrine expression of PDGF-A by epithelial cells engages PDGFR- α in underlying mesenchymal cells to cause mesenchymal cell proliferation (59). A breakdown of epithelial-mesenchymal PDGF signals results in disrupted intestinal morpho-

genesis and epithelial differentiation defects (58). It is currently unclear whether the differentiation defects are secondary to the morphogenetic requirements for PDGF or whether they reflect direct contributions of PDGFR positive mesenchymal cells to epithelial differentiation (58). Although we found that autocrine signals guide Pvr activity, we also found that loss of Pvr results in profound defects in the differentiation program of the intestinal epithelium. Therefore, further studies of the morphogenetic requirements for Pvr signals in ISC differentiation within the *Drosophila* posterior midgut model may illuminate specific requirements for PDGF and VEGF pathway signals in epithelial cell development in mammals.

In addition to developmental roles, deregulation of VEGF and PDGF receptor signals contributes significantly to the generation and progression of numerous cancer types (58). One important hallmark of cancer is growth factor independence (60). In this regard, PDGF has long been recognized as an important autocrine growth factor in the stimulation of neoplastic transformation (58). PDGF/PDGFR proliferative signals promote tumorigenesis in preneoplastic or genetically unstable cells that accumulate genetic changes and become malignant (58). For example, nearly all glioblastomas express a multitude of PDGFs and PDGFRs that establish an autocrine PDGF/PDGFR signal loop (61–63). More recently, autocrine VEGF/VEGFR signals have been directly implicated in cancer progression through the increased renewal of cancer stem cells (64, 65). Given the similarities between Pvr and the established roles of autocrine feedback loop activation of VEGF and PDGF families in cancer progression, we feel that further studies in the genetic regulation of Pvr signals in posterior midgut ISCs provides a fruitful model to study how these pathways promote disease.

Acknowledgments—We thank Bruce Edgar, Pernille Rørth, Benjamin Ohlstein, Xiankun Zeng, Mi-Ae Yoo, and Monica Davis for the fly lines used in this study. Antibodies were generously provided by Pernille Rørth (rat anti-Pvr) and Xiaohang Yang (anti-PDM1). Additional fly lines were obtained through the Bloomington *Drosophila* Stock Center and the Harvard Exelixis Collection. The anti-dl, anti-prospéro, and anti-armadillo monoclonal antibodies were obtained from the Developmental Studies Hybridoma Bank developed under the auspices of the National Institutes of Health, NICHD and maintained by The University of Iowa Department of Biology (Iowa City, IA). The bacterium *Pseudomonas entomophila* was provided by Bruno Lemaître. We are grateful to Andrew Simmonds, Silvia Guntermann, and Brendon Parsons for critical reading of this manuscript.

REFERENCES

1. Reya, T., Morrison, S. J., Clarke, M. F., and Weissman, I. L. (2001) Stem cells, cancer, and cancer stem cells. *Nature* **414**, 105–111
2. Biteau, B., Hochmuth, C. E., and Jasper, H. (2011) Maintaining tissue homeostasis. Dynamic control of somatic stem cell activity. *Cell Stem Cell* **9**, 402–411
3. Morrison, S. J., and Spradling, A. C. (2008) Stem cells and niches. Mechanisms that promote stem cell maintenance throughout life. *Cell* **132**, 598–611
4. Micchelli, C. A., and Perrimon, N. (2006) Evidence that stem cells reside in the adult *Drosophila* midgut epithelium. *Nature* **439**, 475–479
5. Ohlstein, B., and Spradling, A. (2006) The adult *Drosophila* posterior midgut is maintained by pluripotent stem cells. *Nature* **439**, 470–474
6. Apidianakis, Y., and Rahme, L. G. (2011) *Drosophila melanogaster* as a

- model for human intestinal infection and pathology. *Dis. Model Mech.* **4**, 21–30
7. Jiang, H., and Edgar, B. A. (2011) Intestinal stem cells in the adult *Drosophila* midgut. *Exp. Cell Res.* **317**, 2780–2788
 8. Casali, A., and Batlle, E. (2009) Intestinal stem cells in mammals and *Drosophila*. *Cell Stem Cell* **4**, 124–127
 9. Shanbhag, S., and Tripathi, S. (2009) Epithelial ultrastructure and cellular mechanisms of acid and base transport in the *Drosophila* midgut. *J. Exp. Biol.* **212**, 1731–1744
 10. Ohlstein, B., and Spradling, A. (2007) Multipotent *Drosophila* intestinal stem cells specify daughter cell fates by differential notch signaling. *Science* **315**, 988–992
 11. Liu, W., Singh, S. R., and Hou, S. X. (2010) JAK-STAT is restrained by Notch to control cell proliferation of the *Drosophila* intestinal stem cells. *J. Cell. Biochem.* **109**, 992–999
 12. Takashima, S., Adams, K. L., Ortiz, P. A., Ying, C. T., Moridzadeh, R., Younossi-Hartenstein, A., and Hartenstein, V. (2011) Development of the *Drosophila* entero-endocrine lineage and its specification by the Notch signaling pathway. *Dev. Biol.* **353**, 161–172
 13. Xu, N., Wang, S. Q., Tan, D., Gao, Y., Lin, G., and Xi, R. (2011) EGFR, Wingless and JAK/STAT signaling cooperatively maintain *Drosophila* intestinal stem cells. *Dev. Biol.* **354**, 31–43
 14. Jiang, H., Patel, P. H., Kohlmaier, A., Grenley, M. O., McEwen, D. G., and Edgar, B. A. (2009) Cytokine/Jak/Stat signaling mediates regeneration and homeostasis in the *Drosophila* midgut. *Cell* **137**, 1343–1355
 15. Chatterjee, M., and Ip, Y. T. (2009) Pathogenic stimulation of intestinal stem cell response in *Drosophila*. *J. Cell. Physiol.* **220**, 664–671
 16. Buchon, N., Broderick, N. A., Chakrabarti, S., and Lemaitre, B. (2009) Invasive and indigenous microbiota impact intestinal stem cell activity through multiple pathways in *Drosophila*. *Genes Dev.* **23**, 2333–2344
 17. Buchon, N., Broderick, N. A., Kuraishi, T., and Lemaitre, B. (2010) *Drosophila* EGFR pathway coordinates stem cell proliferation and gut remodeling following infection. *BMC Biol.* **8**, 152
 18. Jiang, H., Grenley, M. O., Bravo, M. J., Blumhagen, R. Z., and Edgar, B. A. (2011) EGFR/Ras/MAPK signaling mediates adult midgut epithelial homeostasis and regeneration in *Drosophila*. *Cell Stem Cell* **8**, 84–95
 19. Staley, B. K., and Irvine, K. D. (2010) Warts and Yorkie mediate intestinal regeneration by influencing stem cell proliferation. *Curr. Biol.* **20**, 1580–1587
 20. Ren, F., Wang, B., Yue, T., Yun, E. Y., Ip, Y. T., and Jiang, J. (2010) Hippo signaling regulates *Drosophila* intestine stem cell proliferation through multiple pathways. *Proc. Natl. Acad. Sci. U.S.A.* **107**, 21064–21069
 21. Buchon, N., Broderick, N. A., Poidevin, M., Pradervand, S., and Lemaitre, B. (2009) *Drosophila* intestinal response to bacterial infection. Activation of host defense and stem cell proliferation. *Cell Host Microbe* **5**, 200–211
 22. Jiang, H., and Edgar, B. A. (2009) EGFR signaling regulates the proliferation of *Drosophila* adult midgut progenitors. *Development* **136**, 483–493
 23. Amcheslavsky, A., Jiang, J., and Ip, Y. T. (2009) Tissue damage-induced intestinal stem cell division in *Drosophila*. *Cell Stem Cell* **4**, 49–61
 24. Karpowicz, P., Perez, J., and Perrimon, N. (2010) The Hippo tumor suppressor pathway regulates intestinal stem cell regeneration. *Development* **137**, 4135–4145
 25. Biteau, B., and Jasper, H. (2011) EGF signaling regulates the proliferation of intestinal stem cells in *Drosophila*. *Development* **138**, 1045–1055
 26. Shin, S. C., Kim, S. H., You, H., Kim, B., Kim, A. C., Lee, K. A., Yoon, J. H., Ryu, J. H., and Lee, W. J. (2011) *Drosophila* microbiome modulates host developmental and metabolic homeostasis via insulin signaling. *Science* **334**, 670–674
 27. Shaw, R. L., Kohlmaier, A., Polesello, C., Veelken, C., Edgar, B. A., and Tapon, N. (2010) The Hippo pathway regulates intestinal stem cell proliferation during *Drosophila* adult midgut regeneration. *Development* **137**, 4147–4158
 28. Choi, N. H., Kim, J. G., Yang, D. J., Kim, Y. S., and Yoo, M. A. (2008) Age-related changes in *Drosophila* midgut are associated with PVF2, a PDGF/VEGF-like growth factor. *Aging Cell* **7**, 318–334
 29. Duchek, P., Somogyi, K., Jékely, G., Beccari, S., and Rørth, P. (2001) Guidance of cell migration by the *Drosophila* PDGF/VEGF receptor. *Cell* **107**, 17–26
 30. Cho, N. K., Keyes, L., Johnson, E., Heller, J., Ryner, L., Karim, F., and Krasnow, M. A. (2002) Developmental control of blood cell migration by the *Drosophila* VEGF pathway. *Cell* **108**, 865–876
 31. Fulga, T. A., and Rørth, P. (2002) Invasive cell migration is initiated by guided growth of long cellular extensions. *Nat. Cell Biol.* **4**, 715–719
 32. Munier, A. I., Doucet, D., Perrodou, E., Zachary, D., Meister, M., Hoffmann, J. A., Janeway, C. A., Jr., and Lagueux, M. (2002) PVF2, a PDGF/VEGF-like growth factor, induces hemocyte proliferation in *Drosophila* larvae. *EMBO Rep.* **3**, 1195–1200
 33. Macías, A., Romero, N. M., Martín, F., Suárez, L., Rosa, A. L., and Morata, G. (2004) PVF1/PVR signaling and apoptosis promotes the rotation and dorsal closure of the *Drosophila* male terminalia. *Int. J. Dev. Biol.* **48**, 1087–1094
 34. Ishimaru, S., Ueda, R., Hinohara, Y., Ohtani, M., and Hanafusa, H. (2004) PVR plays a critical role via JNK activation in thorax closure during *Drosophila* metamorphosis. *EMBO J.* **23**, 3984–3994
 35. Brückner, K., Kockel, L., Duchek, P., Luque, C. M., Rørth, P., and Perrimon, N. (2004) The PDGF/VEGF receptor controls blood cell survival in *Drosophila*. *Dev. Cell* **7**, 73–84
 36. Wu, Y., Brock, A. R., Wang, Y., Fujitani, K., Ueda, R., and Galko, M. J. (2009) A blood-borne PDGF/VEGF-like ligand initiates wound-induced epidermal cell migration in *Drosophila* larvae. *Curr. Biol.* **19**, 1473–1477
 37. Sims, D., Duchek, P., and Baum, B. (2009) PDGF/VEGF signaling controls cell size in *Drosophila*. *Genome Biol.* **10**, R20
 38. Bond, D., and Foley, E. (2009) A quantitative RNAi screen for JNK modifiers identifies Pvr as a novel regulator of *Drosophila* immune signaling. *PLoS Pathogens* **5**, e1000655
 39. Park, J. S., Kim, Y. S., and Yoo, M. A. (2009) The role of p38b MAPK in age-related modulation of intestinal stem cell proliferation and differentiation in *Drosophila*. *Aging* **1**, 637–651
 40. Zeng, X., Chauhan, C., and Hou, S. X. (2010) Characterization of midgut stem cell- and enteroblast-specific Gal4 lines in *Drosophila*. *Genesis* **48**, 607–611
 41. Duchek, P., and Rørth, P. (2001) Guidance of cell migration by EGF receptor signaling during *Drosophila* oogenesis. *Science* **291**, 131–133
 42. Furrilli, M., and Bray, S. (2001) A model Notch response element detects Suppressor of Hairless-dependent molecular switch. *Curr. Biol.* **11**, 60–64
 43. Sears, H. C., Kennedy, C. J., and Garrity, P. A. (2003) Macrophage-mediated corpse engulfment is required for normal *Drosophila* CNS morphogenesis. *Development* **130**, 3557–3565
 44. Weber, U., Paricio, N., and Mlodzik, M. (2000) Jun mediates Frizzled-induced R3/R4 cell fate distinction and planar polarity determination in the *Drosophila* eye. *Development* **127**, 3619–3629
 45. Parks, A. L., Cook, K. R., Belvin, M., Dompe, N. A., Fawcett, R., Huppert, K., Tan, L. R., Winter, C. G., Bogart, K. P., Deal, J. E., Deal-Herr, M. E., Grant, D., Marcinko, M., Miyazaki, W. Y., Robertson, S., Shaw, K. J., Tabios, M., Vysotskaia, V., Zhao, L., Andrade, R. S., Edgar, K. A., Howie, E., Killpack, K., Milash, B., Norton, A., Thao, D., Whittaker, K., Winner, M. A., Friedman, L., Margolis, J., Singer, M. A., Kopczyński, C., Curtis, D., Kaufman, T. C., Plowman, G. D., Duyk, G., and Francis-Lang, H. L. (2004) Systematic generation of high-resolution deletion coverage of the *Drosophila melanogaster* genome. *Nat. Genet.* **36**, 288–292
 46. Lee, T., and Luo, L. (2001) Mosaic analysis with a repressible cell marker (MARCM) for *Drosophila* neural development. *Trends Neurosci.* **24**, 251–254
 47. McGuire, S. E., Le, P. T., Osborn, A. J., Matsumoto, K., and Davis, R. L. (2003) Spatiotemporal rescue of memory dysfunction in *Drosophila*. *Science* **302**, 1765–1768
 48. Biteau, B., Hochmuth, C. E., and Jasper, H. (2008) JNK activity in somatic stem cells causes loss of tissue homeostasis in the aging *Drosophila* gut. *Cell Stem Cell* **3**, 442–455
 49. Vodovar, N., Vinals, M., Liehl, P., Basset, A., Degrouard, J., Spellman, P., Bocard, F., and Lemaitre, B. (2005) *Drosophila* host defense after oral infection by an entomopathogenic *Pseudomonas* species. *Proc. Natl. Acad. Sci. U.S.A.* **102**, 11414–11419
 50. Bäckhed, F., Ley, R. E., Sonnenburg, J. L., Peterson, D. A., and Gordon, J. I. (2005) Host-bacterial mutualism in the human intestine. *Science* **307**,

Pvr Regulates *Drosophila* Midgut Homeostasis

- 1915–1920
51. Beebe, K., Lee, W. C., and Micchelli, C. A. (2010) JAK/STAT signaling coordinates stem cell proliferation and multilineage differentiation in the *Drosophila* intestinal stem cell lineage. *Dev. Biol.* **338**, 28–37
 52. McLeod, C. J., Wang, L., Wong, C., and Jones, D. L. (2010) Stem cell dynamics in response to nutrient availability. *Curr. Biol.* **20**, 2100–2105
 53. O'Brien, L. E., Soliman, S. S., Li, X., and Bilder, D. (2011) Altered modes of stem cell division drive adaptive intestinal growth. *Cell* **147**, 603–614
 54. Choi, N. H., Lucchetta, E., and Ohlstein, B. (2011) Nonautonomous regulation of *Drosophila* midgut stem cell proliferation by the insulin-signaling pathway. *Proc. Natl. Acad. Sci. U.S.A.* **108**, 18702–18707
 55. Poernbacher, I., Baumgartner, R., Marada, S. K., Edwards, K., and Stocker, H. (2012) *Drosophila* Pez acts in Hippo signaling to restrict intestinal stem cell proliferation. *Curr. Biol.* **22**, 389–396
 56. Apidianakis, Y., Pitsouli, C., Perrimon, N., and Rahme, L. (2009) Synergy between bacterial infection and genetic predisposition in intestinal dysplasia. *Proc. Natl. Acad. Sci. U.S.A.* **106**, 20883–20888
 57. Biteau, B., Karpac, J., Supoyo, S., Degennaro, M., Lehmann, R., and Jasper, H. (2010) Lifespan extension by preserving proliferative homeostasis in *Drosophila*. *PLoS Genet.* **6**, e1001159
 58. Andrae, J., Gallini, R., and Betsholtz, C. (2008) Role of platelet-derived growth factors in physiology and medicine. *Genes Dev.* **22**, 1276–1312
 59. Karlsson, L., Lindahl, P., Heath, J. K., and Betsholtz, C. (2000) Abnormal gastrointestinal development in PDGF-A and PDGFR- α deficient mice implicates a novel mesenchymal structure with putative instructive properties in villus morphogenesis. *Development* **127**, 3457–3466
 60. Hanahan, D., and Weinberg, R. A. (2000) The hallmarks of cancer. *Cell* **100**, 57–70
 61. Hermansson, M., Nistér, M., Betsholtz, C., Heldin, C. H., Westermark, B., and Funa, K. (1988) Endothelial cell hyperplasia in human glioblastoma. Coexpression of mRNA for platelet-derived growth factor (PDGF) B chain and PDGF receptor suggests autocrine growth stimulation. *Proc. Natl. Acad. Sci. U.S.A.* **85**, 7748–7752
 62. Hermanson, M., Funa, K., Hartman, M., Claesson-Welsh, L., Heldin, C. H., Westermark, B., and Nistér, M. (1992) Platelet-derived growth factor and its receptors in human glioma tissue. Expression of messenger RNA and protein suggests the presence of autocrine and paracrine loops. *Cancer Res.* **52**, 3213–3219
 63. Hermanson, M., Funa, K., Koopmann, J., Maintz, D., Waha, A., Westermark, B., Heldin, C. H., Wiestler, O. D., Louis, D. N., von Deimling, A., and Nistér, M. (1996) Association of loss of heterozygosity on chromosome 17p with high platelet-derived growth factor α receptor expression in human malignant gliomas. *Cancer Res.* **56**, 164–171
 64. Beck, B., Driessens, G., Goossens, S., Youssef, K. K., Kuchnio, A., Caauwe, A., Sotiropoulou, P. A., Loges, S., Lapouge, G., Candi, A., Mascré, G., Drogat, B., Dekoninck, S., Haigh, J. J., Carmeliet, P., and Blanpain, C. (2011) A vascular niche and a VEGF-Nrp1 loop regulate the initiation and stemness of skin tumours. *Nature* **478**, 399–403
 65. Lichtenberger, B. M., Tan, P. K., Niederleithner, H., Ferrara, N., Petzelbauer, P., and Sibilio, M. (2010) Autocrine VEGF signaling synergizes with EGFR in tumor cells to promote epithelial cancer development. *Cell* **140**, 268–279